

Variability in morphology and composition of silica nanoparticles derived from different paddy cultivars

Manpreet Kaur¹ and Anu Kalia^{2,*}

¹Department of Microbiology, College of Basic Sciences and Humanities, and

²Electron Microscopy and Nanoscience Laboratory, Department of Soil Science, College of Agriculture, Punjab Agricultural University, Ludhiana 141 004, India

Turning rice husk (RH) into silica nanoparticles (SiNPs) is a potential strategy for valorization of rice shelling waste. In this study, SiNPs were synthesized from RH of three Basmati (BcvSiNPs) and six Parmal rice varieties (PcvSiNPs) using physico-chemical approach. The average size of BcvSiNPs and PcvSiNPs varied from 20 to 80 nm and 10 to 60 nm respectively, with occurrence of spherical to irregular-shaped aggregates (up to 200 nm) in the former and quasi-spherical to hexagonal shapes in the latter. The SEM-EDS study indicated higher silicon-content in BcvSiNPs compared to PcvSiNPs. However, FTIR analysis of SiNPs accentuated the presence of similar functional groups for both types.

Keywords: Electron microscopy, nanosilica, paddy cultivars, pyrolysis, rice husk, spectroscopy.

RICE is grown across the globe, especially Asia contributes more than 90% of the world pool. Out of a total of 740.96 million tonnes (mt) of paddy (~501.0 mt of milled rice) which was harvested from 158.807 m ha area worldwide, Asia contributed to 692.59 mt paddy from 145.53 m ha paddy-cultivated land in 2017 (FAO statistics; <http://www.fao.org/worldfoodsituation/csdb/en/>). India, the second largest in rice production in the world, had contributed 168.50 mt to the world pool of paddy in 2017 (FAO statistics; <http://www.fao.org/faostat/en/#data/QC>). As rice husk (RH) accounts for ~10% of the grain¹, 16.852 mt RH will be generated posing serious disposal problems due to its low degradability on composting besides less ability to burn under natural conditions².

Rice is known for mining large quantities of silicic acid from the soil, which is deposited in cellular structures of leaf blades and husk by the process of silicification³. RHs are typically 20–22 wt% of the total produce of rice⁴. As RH disposal concerns are rising owing to its large dry volume, low bulk density and high resistance to natural degradation⁵, it incurs additional cost to dispose off tonnes of RH generated annually besides generating pol-

lution, since burning is necessary to decrease the volume of the disposal^{6,7}. Hence, valorization of the waste RH and its utilization for the generation of amorphous silica can possibly help in minimizing waste disposal problems and may enhance remunerations from the waste by-product.

The RH silica content of rice plants varies according to the variety, abiotic factors (soil and climatic conditions, temperature) and agricultural practices followed during cultivation (application of fertilizers and insecticides)⁸. Chemically, RH contains cellulose (40–45%), lignin (25–30%), ash (15–20%), and moisture (8–15%), with ash being mainly comprised of opaline silica (approximately 90–98%)⁴ making it an excellent source of high-grade silica⁸. This potential high-grade silica from RH could be converted to a more useful product, i.e. silica nanoparticles (both amorphous and crystalline) possessing novel nanometre-size dimensions and surface-dependent properties for a myriad of potential applications. Synthesis of nanosilica from RH is economical and may help develop a completely new approach for the synthesis of valuable amorphous silica from a biomass, instead of the energy-intensive process currently adopted by the industry⁵.

The RH-derived silica nanoparticles (SiNPs) are known to be biocompatible and possess ultraviolet (UV) guarding and infrared (IR) reflecting characteristics. These may also exhibit size-dependent fluorescence/luminescent properties which make them attractive tools for new-age nutrition amelioration approaches for enhanced growth and yield in crops⁹, as advanced pesticides¹⁰ and in high-resolution molecular tagging approaches¹¹. The high porosity (pozzolanic nature) and larger surface area properties enable SiNPs to be widely used in adsorbing materials, fillers, pharmaceuticals, catalysts and chromatography columns^{12,13}. Therefore, the present study aims for synthesis of nanosilica from RH as a cheap and environmentally safe silica source. Further, the synthesized particles were characterized by different spectroscopic and microscopic techniques to elucidate variable structural morphologies of diverse rice varieties belonging to Basmati and Parmal groups.

*For correspondence. (e-mail: kaliaanu@pau.edu)

Materials and methods

Synthesis of silica nanoparticles from rice husk

The paddy seeds of nine different varieties – three Basmati, viz. Super Basmati (Sup-Bas), Punjab basmati-2 (PB-2) and Basmati-386 (Bas-386), and six Parmal rice varieties, viz. PR-113, PR-114, PR-115, PR-116, PR-118 and PAU-201 were procured from the Department of Plant Breeding and Genetics, Punjab Agricultural University (PAU), Ludhiana. The procured seeds were first dehusked in a paddy dehusking machine to obtain husk that was ground and treated to synthesize SiNPs according to the method reported by Wang *et al.*⁵, with a few modifications. The method included: boiling of ground RH in 10 wt% HCl solution for 2 h followed by elaborate rinsing with deionized water 5–7 times. The sample was later dried at 100°C for 24 h and dried RH was pyrolyzed in a muffle furnace which was preheated to a predetermined temperature for a certain time (i.e. 700°C for 2 h).

Characterization of silica nanoparticles

Scanning electron microscopy. The SiNPs suspension was prepared by dispensing known amount of dried SiNPs powder in deionized water followed by sonication for 30 min in a bath sonicator (model Toshniwal Ultrasonic Cleaner, India). The morpho-topography of the aggregates was deciphered from 10 µl of the drop-casted SiNPs suspension on carbon tape after vacuum drying to view using scanning electron microscope (SEM) (model Hitachi S-3400N, Japan) operated at 15 kV acceleration voltage in secondary electron imaging mode. The prepared stub was sputter-coated under vacuum pressure of 1.33 Pa, at a current of 18–20 mA for 30 sec exposure of the gold target to obtain 0.01–0.1 µm layer of gold in ion sputter coater (model Hitachi E-1010, Japan). This was performed to curtail the build-up of static charge or charge accumulation on the sample surface during viewing in SEM.

Transmission electron microscopy. The size of the nanoparticles, size distribution and dimensions were determined using transmission electron microscopy (TEM) (model Hitachi H-7650, Japan) of drop-casted SiNPs suspension at 100 kV acceleration voltage in high-contrast/high-resolution zoom-1 imaging mode. All the samples were prepared by placing 10–20 µl of aqueous SiNPs suspension presonicated in a bath ultrasonicator (model SW9H, Toshcon, India) for 25 min and dropped on carbon-coated copper grid (200 mesh size, TedPella, USA). The suspension was incubated for 4–5 min and later excess suspension was removed off the copper grid with a sterilized high-grade absorption filter paper (Whatman filter paper No. 41) followed by air-drying for 5–8 h before imaging using TEM.

UV-Vis spectroscopy. The synthesized silica nanoparticles were subjected to UV absorption spectroscopy in double-beam UV-Vis spectrophotometer (model Elico SL-218, India) using quartz cuvettes with 1.0 cm path length and scanning sample from 200 to 900 nm wavelength range. The absorbance was plotted against wavelength to obtain the absorption peaks for the silica nanoparticles.

Infrared spectroscopy. The vibrational IR spectroscopy was performed for functional group characterization of the synthesized particles and for the elucidation of the fingerprint peaks to confirm the chemistry of the synthesized particles. The dry powder formulation of the synthesized SiNPs was mixed with pre-activated potassium bromide (KBr, Sigma Aldrich, USA) in a 1:100 ratio, and the transparent pellets were obtained by press-pelleting of the homogeneously mixed sample. The prepared pellets were mounted in a pellet moulder and placed in a Fourier transform infrared (FTIR) spectrometer (model Thermo 6700 FT-IR NXRFT Raman module spectrometer, Thermo Electron Scientific Instruments Corporation, Madison, USA) for the mid-IR range from 4000 to 400 cm⁻¹ wavenumbers using XT-KBr-DTGS detector with 32 scans/sample at 0.4 nm resolution.

Scanning electron microscopy–energy dispersive X-ray spectroscopy. The elemental composition in terms of % atom and % weight of elements present on the sample surface was analysed using an energy dispersive X-ray spectroscopy (EDS) module (model Thermo Noran, Thermo Fischer Scientific, MA, USA) attached to the SEM in spectra or point and shoot spectra modes. The samples were analysed using SEM at 15.0 kV acceleration voltage, aperture 2 at minimum 1.0 K magnification. The surface composition was obtained using detector output software and semi-quantitative algorithm (Thermo Noran System Six, Thermo Fischer Scientific, MA, USA) involving least-square fit model utilizing the intensity and pertinent full width half maxima (FWHM) values of the elemental peaks.

Results and discussion

Morphological characterization of silica nanoparticles

Scanning electron microscopy. SEM illustrates occurrence of amorphous silica particles having spherical morphologies with the presence of small to large aggregates (Figure 1). However, paddy variety-dependent variability in the morphology, size and structure of the particles was observed which may be attributed to the variation in the composition of RH further depicting the inherent genetic variation among the source cultivars. The Basmati rice

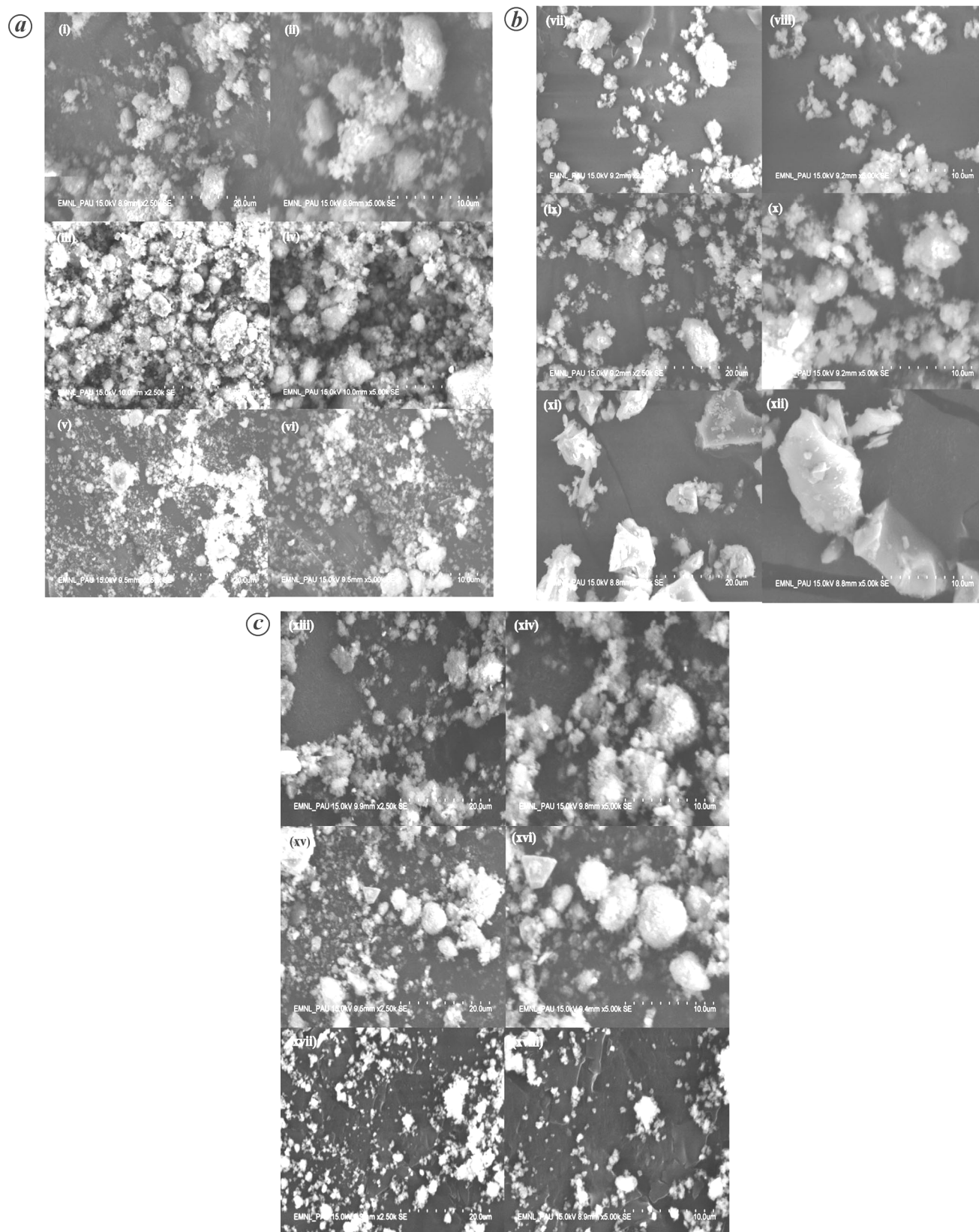


Figure 1. Scanning electron microscopy (SEM) images of silica nanoparticles (SiNP) synthesized from Basmati rice varieties using conventional heating approach at different magnifications. *a*, Sup-Bas at (i) 2.50k and (ii) 5.00k; PB-2 at (iii) 2.50k and (iv) 5.00k; Bas-386 at (v) 2.50k and (vi) 5.00k. *b*, PR-113 at (vii) 2.50k and (viii) 5.00k; PR-114 at (ix) 2.50k and (x) 5.00k; PR-115 at (xi) 2.50k and (xii) 5.00k. *c*, PR-116 at (xiii) 2.50k and (xiv) 5.00k; PR-118 at (xv) 2.50k and (xvi) 5.00k; PAU-201 at (xvii) 2.50k and (xviii) 5.00k.

varieties (BcvSiNPs) exhibited spherical shapes, appeared fluffy/lighter or of lower density, had slightly bigger size and showed greater tendency to form aggregates (Figure 1 *a*). However, all the Parmal rice varieties (PcvSiNPs) had smaller size and exhibited lower aggregation tendency (Figure 1 *b*). Out of the three Basmati varieties, Bas-386 SiNPs (BasSiNPs) showed smaller and less aggregated particles compared to the other two varieties (i.e. Sup-Bas and PB-2). Le *et al.*¹⁴ have obtained similar less-aggregating amorphous SiNPs from Vietnamese RH through sol-gel synthesis using surface-active cetyl amine compound. The PR-116 RH-derived SiNPs had the smallest size among all the six Parmal varieties, followed by PR-113. However, the PR-115 RH-derived SiNPs had a hexagonal, flat, laminated structure, indicating the characteristic tetrahedral silicate unit-cell structure. The prevalence of these nanoparticles indicated complete melting of the opaline silica content of the constituent RH at 700°C, followed by reorganization of SiO₂ molecules to form new structures. Similar hexagonal plate-like structures were also observed in other Parmal rice varieties. This melting and reorganization of the larger aggregates of PcvSiNPs led to greater average diameters. Mechanistically, it may be due to higher potassium content compared to Basmati RHs that led to the presence of residual amounts of potassium in its RH during processing. The residual potassium may have caused mild pre-fusion of the particle surfaces¹⁵.

Transmission electron microscopy. TEM of the synthesized SiNPs showed that majority particles had well-defined, regular, spherical shape with average size ranging from 20 to 70 nm. Similar preparation of spherical SiNPs from RH in the size range 20 to 40 nm has been reported by Yuvakkumar *et al.*¹⁶. However, there was heterogeneity for the remaining SiNPs in terms of sizes as well as shapes. This may be because different varieties were used to synthesize these particles. The size range of BcvSiNPs varied from 20 to 80 nm (Figure 2 *a*). However, the particles got agglomerated forming larger particles of size about 200 nm. Similar results have been reported by other researchers^{14,17,18}. The super basmati RH-derived SiNPs were spherical in shape, porous, appeared to possess corrugated or rough surface, and seemed to be of low density with size ranging from 5 to 100 nm. However, these SiNPs formed large aggregates of size about 150–200 nm. The PB-2 RH-derived SiNPs exhibited spherical shape with smooth surface and individual particle size varying from 30 to 80 nm, besides occurrence of large aggregates of size 100 nm or more. Further, smaller particles of size about 4–7 nm were also observed. The SiNPs derived from Bas-386 RH appeared to have irregular, spherical morphotypes and had the smallest size among all the Basmati varieties. These SiNPs exhibited a wide size variation ranging from 1 to 200 nm, though the average particle size remained in the range 20–50 nm.

The TEM study also indicated their amorphous nature (as exhibited by their lower electron density in bright field TEM imaging mode)¹⁹.

Figure 2 *b* and *c* show TEM images of SiNPs synthesized from different Parmal varieties. Diverse morphologies and shapes were observed for the synthesized PcvSiNPs, probably due to varietal difference among the RHs utilized for preparation of SiNPs. The PcvSiNPs exhibited an average size range of 10–60 nm; however, some particles were even smaller falling in the size range of 2–5 nm. The PR-113 RH-derived SiNPs had quasi-spherical shape and were in the size range 10–150 nm (Figure 2 *b*). These SiNPs showed a tendency to form large agglomerated particles. The SiNPs derived from PR-114 RH were irregular-shaped, with corrugated boundaries resulting in the formation of particle aggregates, though particle size remained in the nanometre range (5–100 nm). However, the SiNPs derived from PR-115 RH were smooth, hexagonal-shaped with size ranging from 10 to 100 nm. These structures may have formed due to complete melting of the opaline silica and partially melted silica forming irregular porous structure. The TEM photomicrographs also depicted the occurrence of SiNPs with size ranging from 1 to 3 nm.

The PR-116 RH-derived particles exhibited different morphologies, including variable irregular shapes spanning over spherical, square-like and hexagonal, and appeared porous and rough-surfaced (Figure 2 *c*). The size ranged from 40 to 100 nm for irregular-shaped particles. However, the size ranged from 10 to 20 nm for hexagonal-shaped crystals. These structures may have formed due to complete melting of opaline silica and partially melted silica forming irregular porous structure. Majority PR-118 RH-derived SiNPs had spherical shape with size in the range 2–4 nm, and average size ranging from 5 to 80 nm. However, these particles formed irregular structures besides showing agglomeration. The PAU-201-derived SiNPs were quasi-spherical while few particles were hexagonal, which may be due to the presence of potassium ions in the RH that catalysed the complete melting of silica and thus the amorphous SiNPs were converted into crystalline phase⁵. The particle size varied from 50 to 100 nm, with some particles lying in range 5–10 nm. These SiNPs also exhibited a tendency to form larger aggregates besides showing porosity.

Spectroscopic analysis

UV-Vis spectroscopy. The UV-Vis spectroscopy was performed to decipher the UV absorption/scattering peaks of the aqueous suspension of SiNPs over the wavelength range 200–800 nm. It can be considered as a cost-effective tool providing information on destabilization of the nanoparticle suspension over time leading to aggregate formation. Figure 3 shows the absorption spectra of

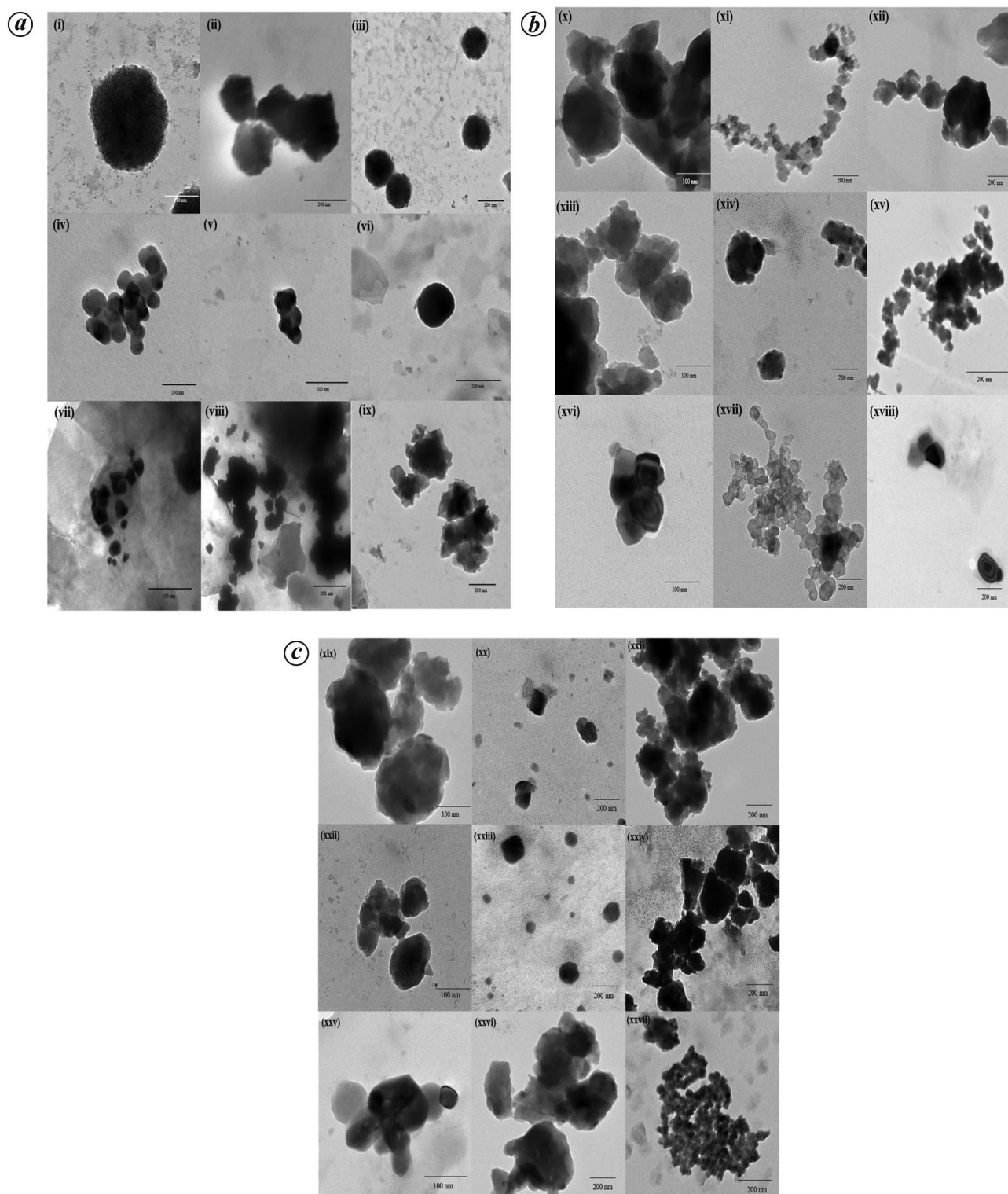


Figure 2. Individual particle morphological diversity of SiNPs derived from rice husk of seven different Basmati and Parmal rice varieties. *a*, Transmission electron microscopy (TEM) images of SiNP synthesized from Basmati rice varieties at different magnifications. Sup-Bas at (i) 40.0k, (ii) 15.0k and (iii) 25.0k; PB-2 at (iv) 40.0k, (v) 15.0k and (vi) 25.0k; Bas-386 at (vii) 40.0k, (viii) 15.0k and (ix) 25.0k. *b*, TEM images of SiNP synthesized from Parmal rice varieties at different magnifications. PR-113 at (x) 40.0k, (xi) 15.0k and (xii) 25.0k; PR-114 at (xiii) 40.0k, (xiv) 15.0k and (xv) 25.0k; PR-115 at (xvi) 40.0k, (xvii) 15.0k and (xviii) 25.0k. *c*, TEM images of SiNP synthesized from Parmal rice varieties at different magnifications. PR-116 at (xix) 40.0k, (xx) 15.0k and (xxi) 25.0k; PR-118 at (xxii) 40.0k, (xxiii) 15.0k and (xxiv) 25.0k; PAU-201 at (xxv) 40.0k, (xxvi) 15.0k and (xxvii) 25.0k.

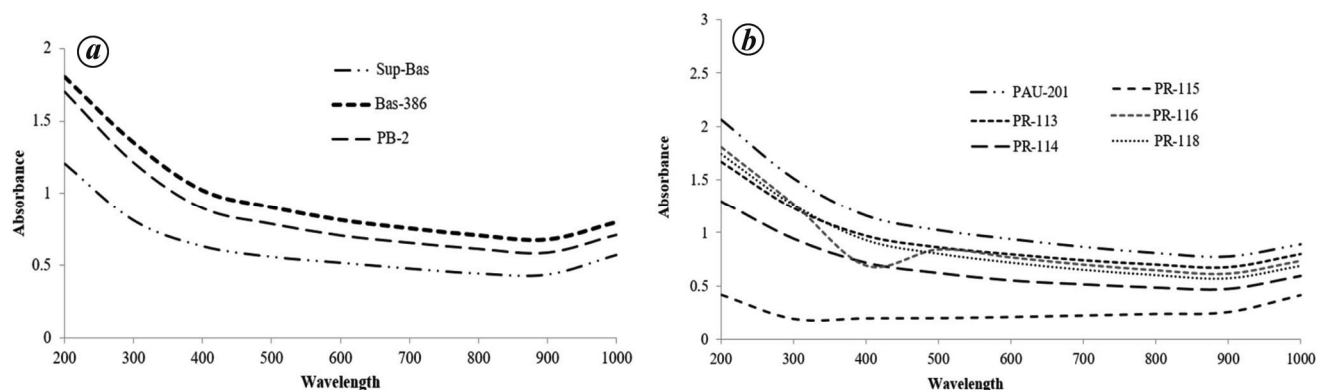


Figure 3. UV-Vis spectra of SiNPs synthesized from (a) Basmati and (b) Parmal rice varieties.

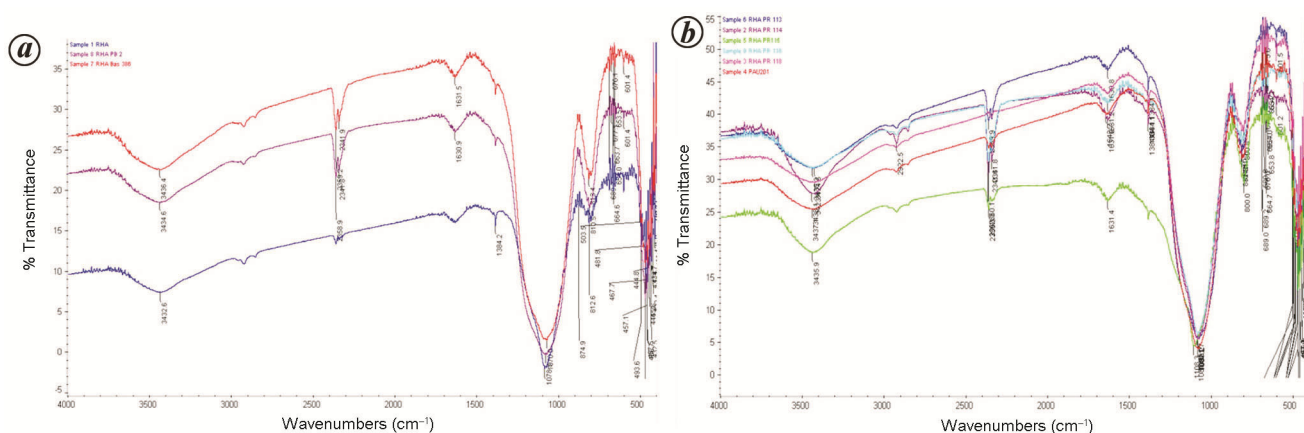


Figure 4. FTIR spectra of SiNPs synthesized from (a) Basmati and (b) Parmal rice varieties.

BcvSiNPs and PcvSiNPs. The synthesized SiNPs exhibited little absorption in the visible wavelength range²⁰. The absorption spectra for all BcvSiNPs did not show any specific variation in the appearance of peaks, except for super basmati SiNPs, which showed a decrease in the range 450–550 nm (Figure 3 a). This may have occurred due to the presence of larger size of the synthesized SiNPs that have elastically scattered the light (Rayleigh scattering) (<http://50.87.149.212/sites/default/files/nano-Composix%20Guidelines%20for%20UV-vis%20Analysis.pdf>). The UV-Vis absorption spectra for all the PcvSiNPs also exhibited occurrence of similar peaks, except for PR-116, for which a peak appeared at 510 nm (Figure 3 b). This peak may have red-shifted contrary to the characteristic peak appearing from 290 to 310 nm for the nanocrystalline silica particles²⁰.

Infrared spectroscopy. The IR spectra BcvSiNPs and PcvSiNPs showed typical IR absorption curves of SiNPs (Figure 4), as reported in several previous studies^{14,17,21–23}. All the Basmati and Parmal RH-derived SiNPs showed occurrence of a peak at 3300–3500 cm^{-1} , which can be

assigned to the O–H stretching vibrations of the surface hydroxyl groups, including the silanol hydroxyl group and the chemisorbed water¹³ (Figure 4 a and b). The contribution of the water molecule can be further confirmed by the presence of absorption band at 1635 cm^{-1} , as a result of the scissor-bending vibration of molecular water^{21,22}. Absorption band(s) appearing around 2400–2500 cm^{-1} correspond to Si–H stretching vibration²³.

The most characteristic is the Si–O–Si stretching vibration peak, which is centred around 1384 cm^{-1} (ref. 17). The absorption bands between 800 and 1260 cm^{-1} can be ascribed as a superimposition of various SiO_2 peaks, Si–OH bonding and peaks due to residual organic groups. The absorption band that appeared around 1100 cm^{-1} indicates Si–O–Si and –C–O–H stretching and –OH deformation, while the peak at 1080 cm^{-1} also indicates the presence of Si–O–Si bond²⁴. Furthermore, diagnostic bands centred around 800 cm^{-1} correspond to the absorption peaks of the Si–O group which result due to symmetric stretching vibration of the Si–O–Si bond^{14,18,22,23,25}. Bands appearing between 400 and 600 cm^{-1} can be related to the bending vibration peak of the Si–O–Si

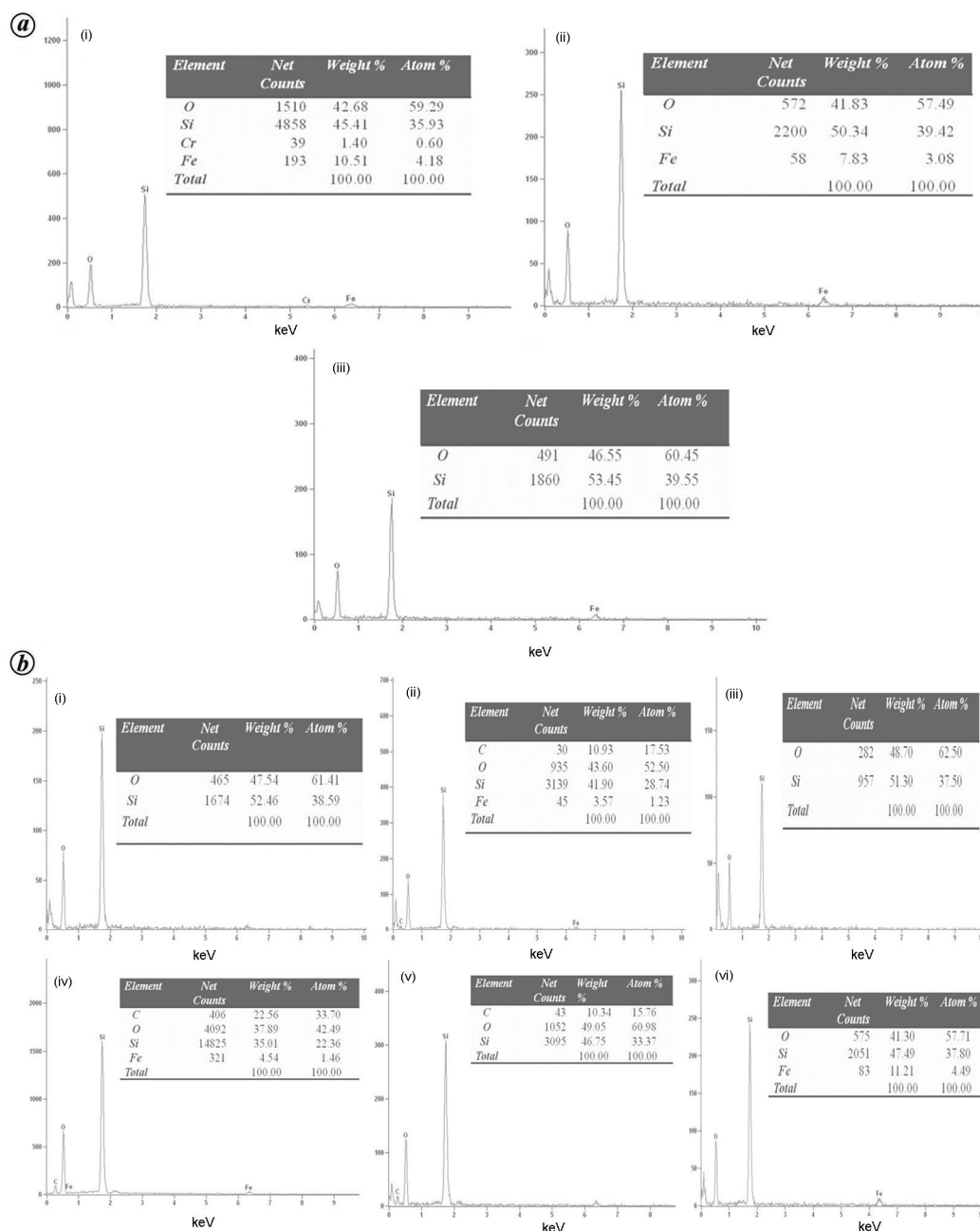


Figure 5. SEM-EDS of SiNPs synthesized from Basmati and Parmal rice varieties. **a**, Silicon signals as observed in the spectra of SiNPs derived from Basmati rice varieties: (i) Sup-Bas, (ii) PB-2 and (iii) Bas-386. **b**, Silicon signals as observed in the spectra of SiNPs derived from Parmal rice varieties: (i) PR-113, (ii) PR-114, (iii) PR-115, (iv) PR-116, (v) PR-118 and (vi) PAU-201.

bond^{18,22,23,25,26}. Another study ascribed the peaks at about 800 and 469 cm^{-1} to Si-H group²⁴. Therefore, FTIR spectrum of the SiNPs synthesized from various RHs indicates the presence of Si-OH and Si-O-Si bonds. The occurrence of these polar functional groups on the SiNPs surface may be responsible for the appreciably high cation exchange and adsorption capabilities²⁴.

Scanning electron microscopy–energy dispersive X-ray spectroscopy. This revealed that the major constituents of

the synthesized SiNPs were silicon and oxygen in % weight and % atom amounts on the sample surface (Figure 5 a and b). The silicon content varied from 45.40 to 53.45 wt% for BcvSiNPs (Figure 5 a) and 41.90 to 52.46 wt% for PcvSiNPs (Figure 5 b). Similarly, oxygen content varied from 41.83 to 46.55 wt% and 43.60 to 48.70 wt% for the BcvSiNPs and PcvSiNPs respectively. Therefore, it can be inferred from SEM–EDS studies that the surface elemental composition of the synthesized nanoparticles shows prevalence of silicon and oxygen

elements. Similar observations for SEM images and EDS signals have been reported by other researchers^{16,17,22,23}.

Conclusion

The silica nanoparticles were successfully synthesized using conventional heating approach from RH of different Basmati and Parmal varieties. The morphology and composition of these SiNPs varied among the two types of rice varieties, with majority SiNPs bearing shapes that differed from spherical in BcvSiNPs, to tubular and hexagonal in PcvSiNPs. This variability may be ascribed to difference in composition of RHs of the varieties. The average size of SiNPs also varied with BcvSiNPs having larger-sized individual as well as aggregate particles compared to PcvSiNPs, particularly the PR-116 RH-derived SiNPs that had the smallest size among six Parmal varieties, followed by PR-113. Surface elemental analysis confirmed the SiO₂ purity of the formed SiNPs to range from 88.09 to 99.79 wt% and 72.90 to 99.70 wt% for the tested Basmati and Parmal rice varieties respectively. This study shows the potential of valorization of waste RH for the synthesis of SiNPs, as it can be an efficient alternative for RH disposal with better economic benefits. It will not only solve the waste-disposal problem of the by-product of the rice shelling industry, but also help to reduce environmental pollution. It can also provide an economical method for the large-scale production of silica.

- Conradt, R., Pimkhaokham, P. and Leela-Adisorn, U., Nanostructured silica from rice husk. *J. Non-Cryst. Solids*, 1992, **145**, 75–79.
- Glushankova, I., Ketov, A., Krasnovskikh, M., Rudakova, L. and Vaisman, I., Rice hulls as a renewable complex material resource. *Resources*, 2018, **7**(2), 1–11.
- Epstein, E., Silicon. *Annu. Rev. Plant Physiol. Plant Mol. Biol.*, 1999, **50**, 641–664.
- Luh, B. S. (ed.), Rice hulls. In *Rice*, Springer, Boston, MA, USA, 1991, pp. 269–294; https://doi.org/10.1007/978-1-4899-3754-4_23
- Wang, W., Martin, J. C., Zhang, N., Ma, C., Han, A. and Sun, L., Harvesting silica nanoparticles from rice husks. *J. Nanopart. Res.*, 2011, **13**, 6981–6990.
- Sun, L. and Gong, K., Silicon-based materials from rice husks and their applications. *Ind. Eng. Chem. Res.*, 2001, **40**, 5861–5877.
- Marchal, J. C., Krug, D. J., McDonnell, P., Sun, K. and Laine, R. M. A., Low cost, low energy route to solar grade silicon from rice hull ash (RHA), a sustainable source. *Green Chem.*, 2015, **17**(7), 3931–3940.
- Ghosh, T. B., Nandi, K. C., Acharya, H. N. and Mukherjee, D., X-ray photoelectron spectroscopic analysis of amorphous silica – a comparative study. *Mater. Lett.*, 1991, **12**, 175–178.
- Karunakaran, G., Suriyaprabha, R., Manivasakan, P., Yuvakkumar, R., Rajendran, V., Prabu, P. and Kannan, N., Effect of nanosilica and silicon sources on plant growth promoting rhizobacteria, soil nutrients and maize seed germination. *IET Nanobiotechnol.*, 2013, **7**(3), 70–77.
- Barik, T. K., Sahu, B. and Swain, V., Nanosilica from medicine to pest control. *Parasitol. Res.*, 2008, **103**, 253–258.
- Liang, S., Shephard, K., Pierce, D. T. and Zhao, J. X., Effects of a nanoscale silica matrix on the fluorescence quantum yield of encapsulated dye molecules. *Nanoscale*, 2013, **5**(19), 9365–9373.
- Bakaev, V. A. and Pantano, C. G., Inverse reaction chromatography: hydrogen/deuterium exchange with silanol groups on the surface of fumed silica. *J. Phys. Chem.*, 2009, **113**, 13894–13898.
- Ahmaruzzaman, M. and Gupta, V. K., Rice husk and its ash as low-cost adsorbents in water and wastewater treatment. *Ind. Eng. Chem. Res.*, 2011, **50**(24), 13589–13613.
- Le, V. H., Thuc, C. N. H. and Thuc, H. H., Synthesis of silica nanoparticles from Vietnamese rice husk by sol–gel method. *Nanoscale Res. Lett.*, 2013, **8**, 58.
- Fernandes, I. J., Calheiro, D., Sánchez, F. A. L., Camacho, A. L. D., Rocha, T. L. A., Moraes, C. A. M. and de Sousa, V. C., Characterization of silica produced from rice husk ash: comparison of purification and processing methods. *Mater. Res.*, 2017, **20**(Suppl. 2), 512–518.
- Yuvakkumar, R., Elango, V., Rajendran, V. and Kannan, N., High-purity nano silica powder from rice husk using a simple chemical method. *J. Exp. Nanosci.*, 2014, **9**, 272–281.
- Nittaya, T. and Apinon, N., Preparation of nanosilica powder from rice husk ash by precipitation method. *Chiang Mai J. Sci.*, 2008, **35**(1), 206–211.
- Njiomou, D. C., Mlowe, S., Njopwouo, D. and Revaprasadu, N., One-step synthesis of silica nanoparticles by thermolysis of rice husk ash using nontoxic chemicals ethanol and polyethylene glycol. *J. Appl. Chem.*, 2015, **4**(4), 1218–1226.
- Stathers, T. E., Denniff, M. and Golob, P., The efficacy and persistence of diatomaceous earths admixed with commodity against four tropical stored product beetle pests. *J. Stored Prod. Res.*, 2004, **40**, 113–123.
- Venkateswaran, S., Yuvakkumar, R. and Rajendran, V., Nano silicon from nano silica using natural resource (RHA) for solar cell fabrication. *Phosphorus, Sulfur Silicon Relat. Elem.*, 2013, **188**(9), 1178–1193.
- Essien, E. R., Olaniyi, O. A., Adams, L. A. and Shaibu, R. O., Sol–gel-derived porous silica: economic synthesis and characterization. *J. Miner. Mater. Character Eng.*, 2012, **11**, 976–981.
- Rida, M. A. and Harb, F., Synthesis and characterization of amorphous silica nanoparticles from aqueous silicates using cationic surfactants. *J. Metal. Mater. Miner.*, 2014, **24**, 37–42.
- Sivasubramanian, S. and Sravanthi, K., Synthesis and characterization of silica nanoparticles from coconut shell. *Int. J. Pharm. Biol. Sci.*, 2015, **6**, 530–536.
- Srivastava, V. C., Mall, I. D. and Mishra, I. M., Characterization of mesoporous rice husk ash (RHA) and adsorption kinetics of metal ions from aqueous solution onto RHA. *J. Hazard. Mater.*, 2006, **134**(1–3), 257–267.
- Premaratne, W. A. P. J., Priyadarshana, W. M. G. I., Gunawardena, S. H. P. and Alwis, A. A. P. D., Synthesis of nanosilica from paddy husk ash and their surface functionalization. *J. Sci. Univ. Kelaniya*, 2013, **8**, 33–48.
- Guo, Y., Wang, M., Zhang, H., Liu, G., Zhang, L. and Qu, X., The surface modification of nanosilica, preparation of nanosilica/acrylic core–shell latex and its application in toughening PVC matrix. *J. Appl. Polym. Sci.*, 2008, **107**, 2671–2680.

ACKNOWLEDGEMENTS. The second author thank the Indian Council of Agricultural Research, New Delhi for providing financial assistance through a project under the Nanotechnology Platform. We thank Dr V. R. Parshad (Ex-Director, Electron Microscopy and Nanoscience Laboratory, College of Agriculture, PAU, Ludhiana) for his valuable suggestions that helped in the conceptualization of this work.

Received 21 October 2016; revised accepted 17 April 2020

doi: 10.18520/cs/v119/i2/335-342